

First-Principles Study of Elasticity and Electronic Structure of Incompressible Osmium Diboride

Z. F. Hou*

Department of Physics, Fudan University, Shanghai, P. R. China 200433

(Dated: September 26, 2018)

Abstract

Recently, osmium diboride (OsB_2) has attracted considerable attention as an incompressible and hard material. We investigate the structural property, elastic constant, and electronic structure of orthorhombic OsB_2 by the first-principles total energy calculations. The calculations are performed within the density functional framework using the projector augmented plane wave method. The structural property and bulk modulus of OsB_2 compare well with experimental data. The nine independent elastic constants of orthorhombic OsB_2 at zero-pressure have also been calculated by symmetry-general least-squares extraction method. We have analyzed the mechanical stability of orthorhombic OsB_2 in term of the calculated elastic constants. A detailed study of the electronic structure and the charge-density redistribution reveals the features of strong covalent B-B and Os-B bondings in orthorhombic OsB_2 . The orbital hybridization and the characteristics of bonding orbitals in OsB_2 are identified. Orthorhombic OsB_2 exhibits a metallic character and the states at Fermi level mainly come from the d orbital of Os atoms.

*Electronic address: zfhou@fudan.edu.cn

I. INTRODUCTION

To design and explore ultrahard materials is of great scientific and practical interest in both experimental and theoretical studies [1, 2, 3, 4, 5, 6], because the class of hard materials has a wide variety of important technological applications ranged from cutting and polishing tools to wear-resistant coating [2, 5, 7]. Stiffness reflects the elastic compressibility of materials, which is related to the bulk modulus, shear modulus, and the Young's modulus. Hardness describes the resistance of materials to plastic deformation [6]. It is recognized that there is a good correlation between shear modulus and hardness [2, 3, 8] and a three-dimensional network composed of short, strong bonds is critical for hardness of material [6]. Many synthetic and theoretical efforts are made to design new ultrahard materials in past decades and two main approaches have been summarized [6] as the following: a) combination of light elements (such as boron, nitrogen, and/or oxygen) to form short covalent bonds and b) compounding of elements with very high densities of valence electrons to ensure that the materials resist being squeezed together. Cubic BC_2N , an example of the first approach, was synthesized as a dense ternary phase in the B–C–N system [7] and found to be an extreme hardness second only to diamond [7, 9]. For the second approach, one usually uses transition metals having a high bulk modulus but low hardness to combine with small, covalent bond-forming atoms [6]. For example, highly incompressible phase of RuO_2 [10] owes to a strong covalent bonding between ruthenium d states and oxygen p states [11].

Other representative example for the second approach is the compounds related osmium (Os) element. The pure Os metal was measured to have a high bulk modulus of 462 GPa [12], 411 ± 6 GPa [13], and 395 ± 15 GPa [14] by different experimental methods, but found to have a low hardness of only 400 kg/mm² [15]. These features of could be understand that [6] the high bulk modulus of Os mainly owes to the high valence electron density ($0.572 e/\text{\AA}^3$) and the low hardness of Os metal with hexagonal close-packed crystal structure is related to the metallic bonding character. To improve the hardness of osmium, incorporation of small and covalent main group elements (such as boron, carbon, nitrogen, and/or oxygen) into osmium metal has been proposed in experimental and theoretical studies [6, 11, 16, 17]. OsO_2 is expected to have a covalent bonding and a high bulk modulus [11], analogous to RuO_2 . Although OsC and OsN compounds are not yet synthesized successfully, recent *ab initio* calculations predict that [16] OsC in hexagonal WC structure has a bulk modulus

of 396 GPa and is a promising superhard material. For one of binary compounds in Os-B system, OsB₂, recent experiment measures show that [17] OsB₂ is an ultra-incompressible and hard material with bulk modulus of 365-395 GPa and hardness of ≥ 2000 kg/mm².

In order to investigate the mechanical properties of OsB₂ and understand its high stiffness and hardness, we have evaluated the nine independent elastic constants including bulk modulus and shear modulus of OsB₂ using *ab initio* pseudopotential calculations. Our results show that the behavior of this compound can be understood on a fundamental level in terms of their electronic band structure. The unusual hardness originates from the strong covalent bonding character between the *p* bonding states of boron atoms and the *d* orbitals of osmium atom, and the strong covalent bonding between boron and boron atoms. The ultra-incompressibility exhibits anisotropy ($C_{33} > C_{11} > C_{22}$), which is due to the different bonding character of interlayer along *c*, *a*, and *b*-directions of crystal.

II. METHOD

Because crystals deform almost in a linear elastic manner at small strains, the increment of strain energy density of a homogeneous and elastically deformed crystal is given by

$$dE = \sigma_{ij}d\epsilon_{ij} \quad (1)$$

where σ_{ij} are the elements of stress tensor and ϵ_{ij} are the elements of strain tensor. Indices *i*, *j*, *k* and *l* run from 1 to 3. Elastic constants are defined as

$$c_{ijkl} \equiv \frac{\partial \sigma_{ij}}{\partial \epsilon_{ij}} = \frac{1}{V} \frac{\partial^2 E}{\partial \epsilon_{ij} \partial \epsilon_{kl}} - \delta_{ij} \sigma_{kl} = C_{ijkl} - \delta_{ij} \sigma_{kl} \quad (2)$$

where *V* and δ are the volume of the unstrained crystal and Kronecker delta function, respectively. At zero hydrostatic pressure $c_{ijkl} = C_{ijkl}$. The internal energy $E(V, \{\epsilon_{ij}\})$ of a crystal under a general strain ϵ_{ij} can be expressed by expanding the internal energy $E(V)$ of the deformed crystal with respect to the strain tensor, as

$$E(V, \{\epsilon_{ij}\}) = E(V, 0) + V \sum_{i,j=1}^3 \sigma_{ij} \epsilon_{ij} + \frac{V}{2} \sum_{i,j,k,l=1}^3 C_{ijkl} \epsilon_{ij} \epsilon_{kl} + \dots \quad (3)$$

where $E(V, 0)$ is the corresponding ground state energy. If one uses Voigt notation ($xx \rightarrow 1$, $yy \rightarrow 2$, $zz \rightarrow 3$, $yz \rightarrow 4$, $xz \rightarrow 5$ and $xy \rightarrow 6$) for the strain tensors subscripts (ij, kl) in

the the above expression, Eq. (3) can be rewritten as

$$E(V, \{\epsilon_i\}) = E(V, 0) + V \sum_{i=1}^6 \sigma_i e_i + \frac{V}{2} \sum_{i,j=1}^6 C_{ij} e_i e_j + \dots \quad (4)$$

with the strain tensor

$$\epsilon = \begin{pmatrix} e_1 & \frac{1}{2}e_6 & \frac{1}{2}e_5 \\ \frac{1}{2}e_6 & e_2 & \frac{1}{2}e_4 \\ \frac{1}{2}e_5 & \frac{1}{2}e_4 & e_3 \end{pmatrix} \quad (5)$$

Therefore, one can apply small elastic strains and calculate the change of energy or stress to obtain elastic constants. Direct calculation of elastic constants are possible from first-principles total energy calculations and symmetry-general least-squares extraction method [18]. The independent elastic constants for crystals can be determined by selectively imposing strains either individually or in combination along specific crystallographic directions [19, 20, 21, 22, 23]. Table I illustrates the deformations employed in determining independent elastic constants of orthorhombic crystal [19, 20].

First-principles total energy calculations on OsB₂ were performed using a plane-wave pseudopotential method as implemented in the VASP code [24, 25]. The exchange-correlation energy functional was treated with the local density approximation (LDA) given by Ceperley and Alder [26] as parameterized by Perdew and Zunger [27]. Electron-ion interaction was represented by the projector augmented wave (PAW) method [28, 29] and wave functions were expanded by the plane waves up to an energy cutoff of 500 eV. Brillouin-zone integrations were approximated using the special k -point sampling of Monkhorst-Pack scheme [30] with a $9 \times 13 \times 9$ grid. The total energy convergence test showed that convergency to within 1 meV/atom was achieved with the above calculation parameters. The bulk unit cell lattice vectors and atomic coordinates of orthorhombic OsB₂ were relaxed at a series of fixed volumes by optimizing both the forces and stresses. The residual force and stress in the equilibrium geometry are of the order of 0.01 eV/Å and 10^{-3} GPa, respectively. The obtained energies were fitted with the third-order Birch-Murnaghan equation of state (EOS) [31] to give the equilibrium volume and the minimum energy. The final calculated cell parameters are given in Table II, which are in good agreement with the available experimental values.

III. RESULTS AND DISCUSSIONS

A. Structural properties

The single-crystal of OsB₂ was found to have the orthorhombic symmetry with the space group *Pmmn* (No. 59) and lattice constants $a = 4.6832 \text{ \AA}$, $b = 2.8717 \text{ \AA}$ and $c = 4.0761 \text{ \AA}$, using the polycrystalline *x*-ray diffraction techniques.[32] In the orthorhombic unit cell of OsB₂, the Os atoms were determined at the Wyckoff position of $2a (\frac{1}{4}, \frac{1}{4}, z)$ and $4f (u, \frac{1}{4}, v)$ for B atoms [32]. The crystal structure of OsB₂ is illustrated in Fig.1, especially, the layer structure repeated along *c*-(or *z*-)direction with Os-B-B-Os sandwich structure is also shown. The orthorhombic unit cell of OsB₂ contains two formula unit (f.u.). The calculated lattice constant are $a = 4.6444 \text{ \AA}$, $b = 2.8505 \text{ \AA}$ $c = 4.0464 \text{ \AA}$, which are in good agreement with the available experiment values [32] and previous spin polarized LDA (namely, LSDA) calculation results ($a= 4.6433 \text{ \AA}$, $b = 2.8467 \text{ \AA}$ $c = 4.0432 \text{ \AA}$) [33]. We should pointed out that we have also performed the spin polarized LDA calculation on OsB₂ and found that there is no difference between the results of LDA and LSDA. The calculated volume ($53.57 \text{ \AA}^3/\text{f.u.}$) is 2.2% smaller than experimental value, which is typical for the LDA approximation to DFT. The calculated atomic coordinate parameters are $z = 0.1538$ for Os atoms, $u = 0.0588$ and $v = 0.6378$ for B atoms. We have also calculated the equation of state (the pressure versus volume) by taking the volume derivative of the fitted total energy obtained from our LDA calculation, the result along the available experimental data is shown in Fig. 2. The bulk modulus and its pressure derivative for OsB₂, obtained by fitting the total energy curve to third-order Birch-Murnaghan equation of state (EOS) [31], are 336.1 GPa and 4.27 in our LDA calculations. This bulk modulus is 7.9% ~ 15% smaller than the experimental value (365-395 GPa) [17]. Note that the corresponding derivative of bulk modulus to pressure in experimental studies [17] is fixed in the range between 4 and 1.4. In order to further asses the effects of the exchange-correlation approximation, we have also studied structural properties of OsB₂ using the generalized gradient approximation (GGA) [34]. GGA consistently yields a larger volume than experiment, while LDA consistently gives a smaller volume than GGA (see Table II). Since the GGA calculation gives a smaller bulk modulus (303.45 GPa) of OsB₂ than the experimental data, in the following sections we will mainly present and discuss the results obtained by LDA calculations.

B. Elastic constants

The nine independent elastic constants for OsB₂ were determined by imposing three different strains given in Table I on the equilibrium lattice of orthorhombic unit cell and fitting the dependence of the resulting change in energy on the strain. Up to seven deformations, γ from -0.009 to 0.009 in steps of 0.003, were applied to determine each elastic constant. The ground state energies of OsB₂ unit cell were determined for all these deformation strains. The $E(\gamma)$ curves are well fitted by the third-order polynomials in γ (Eq.(4)), as can be seen from the small standard errors in the calculated C_{ij} . The elastic constants were then calculated using the energy relations listed in Table I. During the calculations on all elastic constants of orthorhombic OsB₂, relaxation of the coordinate of ions in the strained lattice was carried out for achieving accurate results. The nine independent elastic constants for orthorhombic OsB₂ are listed in Table III, which experimental data on elasticity is not available, except for bulk modulus. The nine independent elastic constants of orthorhombic OsB₂ are $C_{11} = 597.0$ GPa, $C_{12} = 198.1$ GPa, $C_{13} = 206.1$ GPa, $C_{22} = 581.2$ GPa, $C_{23} = 142.6$ GPa, $C_{33} = 825.0$ GPa, $C_{44} = 70.1$ GPa, $C_{55} = 212.0$ GPa, and $C_{66} = 201.3$ GPa in our calculations.

Under the Voigt approximation [19, 35], the elastic constants for polycrystalline aggregates are described by Voigt shear modulus (G_V) and Voigt bulk modulus (B_V). For the orthorhombic lattice, G_V and B_V are expressed in the following equations [19]:

$$G_V = \frac{1}{15}(C_{11} + C_{22} + C_{33} - C_{12} - C_{13} - C_{23}) + \frac{1}{5}(C_{44} + C_{55} + C_{66}) \quad (6)$$

$$B_V = \frac{1}{9}(C_{11} + C_{22} + C_{33} + 2C_{12} + 2C_{13} + 2C_{23}). \quad (7)$$

The calculated Voigt shear constant of OsB₂ is about 193.8 GPa. The Voigt bulk modulus calculated from the theoretical values of the elastic constants is 344.1 GPa. It agrees well with the one extracted from the fit to the third-order Birch-Murnaghan equation of state, 336.1 GPa. Since the Young's modulus (E) and Poisson's ratio (ν) for an isotropic materials can be obtained from the following relations [19, 36]:

$$E = \frac{9BG}{3B + G} \quad (8)$$

$$\nu = \frac{3B - 2G}{2(3B + G)}. \quad (9)$$

The calculated Young's modulus and Poisson's ratio of OsB₂ are 489.5 GPa and 0.263, respectively.

The requirement of mechanical stability in a orthorhombic crystal leads to the following restrictions on the elastic constants:[20, 36]

$$\begin{aligned}
(C_{11} + C_{22} - 2C_{12}) &> 0, \\
(C_{11} + C_{33} - 2C_{13}) &> 0, \\
(C_{22} + C_{33} - 2C_{23}) &> 0, \\
C_{11} > 0, C_{22} > 0, C_{33} > 0, \\
C_{44} > 0, C_{55} > 0, C_{66} > 0, \\
(C_{11} + C_{22} + C_{33} + 2C_{12} + 2C_{13} + 2C_{23}) &> 0.
\end{aligned} \tag{10}$$

Since B_0 is a weighted average of C_{ii} and C_{ij} (indices i and j running from 1 to 3), these conditions also lead to a restriction on the magnitude of B_0 . Namely, B_0 is required to be intermediate in value between $\frac{1}{3}(C_{12} + C_{13} + C_{23})$ and $\frac{1}{3}(C_{11} + C_{22} + C_{33})$ [20, 36],

$$\frac{1}{3}(C_{12} + C_{13} + C_{23}) < B_0 < \frac{1}{3}(C_{11} + C_{22} + C_{33}) \tag{11}$$

The elastic constants of orthorhombic OsB₂ in Table III obey these stability conditions (Eq.(10) and (11)). In particular, C_{12} is smaller than the average of C_{11} and C_{22} , C_{13} is smaller than the average of C_{11} and C_{33} , C_{23} is smaller than the average of C_{22} and C_{33} , and the bulk modulus is smaller than the average of C_{11} , C_{22} , and C_{33} but larger than the average of C_{12} , C_{13} , and C_{23} .

C. Electronic structures and analysis of chemical bonding

The energy band structure and density of states (DOS) (including total, site and angular momentum decomposed DOS) of orthorhombic OsB₂ are shown in Fig. 2 and 3, respectively. It evidently exhibits a metallic character. The valence bands in Fig. 2 have a width of about 15 eV, and are split into two disjointed groups, respectively. The lower group has a width of about 5 eV and the upper one up to the Fermi level (E_F) has a width of about 10 eV. Combining from the DOS figures (3), the lower group in the energy range between -15 eV and -10 eV below the Fermi level (E_F) is largely contributed by B-2s levels and small amount of Os-6s, the upper one in the energy range from -12 eV to E_F is mainly composed by Os-5d

orbitals and B-2*p*. It suggests that the strong hybridization between B-2*p* and Os-5*d* orbitals occur below the Fermi level. Additionally, *d* orbitals of Os atom are contributed most to the total DOS at E_F . These findings are consistent with the previous studies on electronic structure of OsB₂ [33, 37].

The large values and anisotropy of elastic constants of OsB₂ can be understood by examining the nature of chemical bonding between the atoms. In order to understand the bonding between the Os-B, Os-Os, and B-B atoms, the lines charge density along nearest neighbor Os–B, Os–Os, B–B atoms are illustrated in Fig. 5. It is clearly seen that charge highly accumulates around Os atom, and Os-B, Os-Os and B-B bondings exhibit covalent, metallic, covalent characters, respectively. It also supported by above discussion that the *d* states of Os atoms and *p* states of B atoms have a strong hybridization seen in density of states. In order to further reveal the topology of Os-Os, Os-B and the B-B bondings, we illustrate the contour plots of electron density in different crystallographic planes. Fig. 6 illustrates the two-dimensional electron charge density distribution in the planes with normal vector along $\langle 100 \rangle$, $\langle 010 \rangle$ and $\langle 001 \rangle$, respectively. From Fig. 6(a) and (d), in which planes with the normal vector along $\langle 100 \rangle$ and central point at Os1 atom ($\frac{1}{4}, \frac{1}{4}, z$), and with the normal vector along $\langle 001 \rangle$ and central point at Os1 atom, respectively, it can be clearly seen that there is no strong bonding between Os–Os atoms as there is no accumulation of charges in excess of the background charge density of the plane. It appears that the Os–Os bonding is predominantly metallic in OsB₂. Fig. 6(e) and (f), in which planes with the normal vector along $\langle 001 \rangle$ and central point at B1 atom ($u, \frac{1}{4}, v$), and through B1, B2, B3 and B4 atoms, respectively, It also can be clearly seen that there is strong covalent bonding between B-B atoms. The nature of Os-B and B-B bonding is illustrated in Fig. 6(c) of the two-dimensional contour electron density map with normal vector along $\langle 010 \rangle$ and central point at Os1 atom ($\frac{1}{4}, \frac{1}{4}, z$). It can be seen that there is a charge accumulation of electron charge between the Os-B atoms, which is consistent with the idea of B-2*p* and Os-5*d* hybridization noted in Fig. 4. This also clearly confirms both B-B and Os-B bondings are covalent character. Because the orthorhombic OsB₂ is stacked by Os-B-B-Os atomic layer structures in the *c* (or *z*) direction of crystal, these mean that the atom bondings of interlayer are strong covalent characters of Os-B and B-B. This also explains the high value of elastic constant C_{33} (825.0 GPa) and a relatively lower value of elastic constant C_{11} (597.0 GPa) and C_{22} (581.2 GPa).

IV. CONCLUSIONS

The structural parameters, elastic constants, and electronic structures of OsB₂ have been calculated and analyzed. Our calculated structural parameters including the lattice constants and internal parameters are in good agreement with the experiment data. The LDA calculations yielded the bulk modulus (336.1 GPa) of OsB₂, which is more close to the experimental data than that of GGA calculations (303.45 GPa). The LDA calculations also predicted that the independent elastic constants of OsB₂ are $C_{11} = 597.0$ GPa, $C_{12} = 198.1$ GPa, $C_{13} = 206.1$ GPa, $C_{22} = 581.2$ GPa, $C_{23} = 142.6$ GPa, $C_{33} = 825.0$ GPa, $C_{44} = 70.1$ GPa, $C_{55} = 212.0$ GPa, and $C_{66} = 201.3$ GPa, respectively. The incompressibility of OsB₂ exhibits anisotropy ($C_{33} > C_{11} > C_{22}$) and the *c*-direction of crystal is the least compressible due to the difference of atom bonding character of interlayer along different crystalline planes. The detailed study of the electronic structure and charge density redistribution reveals the strong covalent Os-B atoms bonding and B-B atoms bonding play a important role in the incompressibility and hardness of OsB₂.

V. ACKNOWLEDGEMENTS

The author acknowledge support from Shanghai Postdoctoral Science Foundation under Grant No. 05R214106. The computation was performed at Supercomputer Center of Fudan. The XCRYSDEN package [38] and LEV00 code [39] were used for generation of ball-and-stick model and calculation of charge density maps, respectively.

-
- [1] S. Vepřek, J. Vac. Sci. Tech. A **17**, 2401 (1999).
 - [2] V. V. Brazhkin, A. G. Lyapin, and R. J. Hemley, Philos. Mag. A **82**, 231 (2002).
 - [3] J. Haines, J. M. Leger, and G. Bocquillon, Annu. Rev. Mater. Res. **31**, 1 (2001).
 - [4] A. L. Liu and M. L. Cohen, Science **245**, 841 (1989).
 - [5] S. H. Jhi, J. Ihm, S. G. Louie, and M. L. Cohen, Nature **399**, 132 (1999).
 - [6] R. B. Kaner, J. J. Gilman, and S. H. Tolbert, Science **308**, 1268 (2005).
 - [7] V. L. Solozhenko, D. Andrault, G. Fiquet, M. Mezouar, and D. C. Rubie, Appl. Phys. Lett. **78**, 1385 (2001).

- [8] D. M. Teter, Mater. Res. Soc. Bull. **23**, 22 (1998).
- [9] Y. Zhang, H. Sun, and C. F. Chen, Phys. Rev. Lett. **93**, 195504 (2004).
- [10] J. Haines and J. M. Léger, Phys. Rev. B **48**, 13344 (1993).
- [11] U. Lundin, L. Fast, L. Nordström, B. Johansson, J. M. Wills, and O. Eriksson, Phys. Rev. B **57**, 4979 (1998).
- [12] H. Cynn, J. E. Klepeis, C. S. Yoo, and D. A. Young, Phys. Rev. Lett. **88**, 135701 (2002).
- [13] F. Occelli, D. L. Farber, J. Badro, C. M. Aracne, D. M. Teter, M. Hanfland, B. Canny, and B. Couzinet, Phys. Rev. Lett. **93**, 095502 (2004).
- [14] K. Takemura, Phys. Rev. B **70**, 012101 (2004).
- [15] J. F. Shackelford and W. Alexander, *CRC Handbook of Materials Science & Engineering* (CRC Press, Boca Raton, FL, 2001), 3rd ed.
- [16] J. C. Zheng, Phys. Rev. B **72**, 052105 (2005).
- [17] R. W. Cumberland, M. B. Weinberger, J. J. Gilman, S. M. Clark, S. T. Tolbert, and R. B. Kaner, J. Am. Chem. Soc. **127**, 7264 (2005).
- [18] Y. L. Page and P. Saxe, Phys. Rev. B **65**, 104104 (2002).
- [19] P. Ravindran, L. Fast, P. A. Korzhavyi, B. Johansson, and J. Wills, J. Appl. Phys. **84**, 4891 (1998).
- [20] O. Beckstein, J. E. Klepeis, G. L. W. Hart, and O. Pankratov, Phys. Rev. B **63**, 134112 (2001).
- [21] M. Mattesini, R. Ahuja, and B. Johansson, Phys. Rev. B **68**, 184108 (2003).
- [22] P. Ravindran, P. Vajeeston, R. Vidya, A. Kjekshus, and H. Fjellvåg, Phys. Rev. B **64**, 224509 (2001).
- [23] G. S.-Neumann, L. Stixrude, and R. E. Cohen, Phys. Rev. B **60**, 791 (1999).
- [24] G. Kresse and J. Furthmüller, Comput. Mater. Sci. **6**, 15 (1996).
- [25] G. Kresse and J. Furthmüller, Phys. Rev. B **54**, 11169 (1996).
- [26] D. M. Ceperley and B. J. Alder, Phys. Rev. Lett. **45**, 566 (1980).
- [27] J. P. Perdew and A. Zunger, Phys. Rev. B **23**, 5048 (1981).
- [28] P. E. Blöchl, Phys. Rev. B **50**, 17953 (1994).
- [29] G. Kresse and J. Joubert, Phys. Rev. B **50**, 1758 (1999).
- [30] H. J. Monkhorst and J. D. Pack, Phys. Rev. B **13**, 5188 (1976).
- [31] F. Birch, Phys. Rev. **71**, 809 (1947).

- [32] R. B. Roof and C. P. Kempter, *J. Chem. Phys.* **37**, 1473 (62).
- [33] Z. Y. Chen, H. J. X. adn J. L. Yang, J. G. Hou, and Q. S. Zhu, cond-mat/0508506 (2005), unpublished.
- [34] J. P. Perdew and Y. Wang, *Phys. Rev. B* **45**, 13244 (1992).
- [35] W. Voigt, *Lehrbuch der Kristallphysik* (Taubner, Leipzig, 1928).
- [36] G. Grimvall, *Thermophysical properties of materials* (Elsevier/North-Holland, Amsterdam, 1999), enlarged and revised ed.
- [37] A. L. Ivanovskii and N. I. Medvedeva, *Russian J. Inorg. Chem.* **44**, 1633 (1999).
- [38] A. Kokalj, *J. Mol. Graphics Modelling* **17**, 176 (1999), Code available from <http://www.xcrysden.org/>.
- [39] L. N. Kantorovich, *User-friendly visualisation program for plane-wave ab initio DFT codes CASTEP/CETEP/VASP*, unpublished (1996-2002).
- [40] The label and position of high symmetry k points for space group $Pmmn$ (No. 59) can be found in http://www.cryst.ehu.es/cryst/get_kvec.html.

TABLE I: Parametrization of the strains used to calculate the elastic constants of orthorhombic OsB₂. The energy expressions reported on the third column refer to Eq. 4.

Strain	Parameters (unlisted $e_i = 0$)	$\Delta E/V$ in $O(\gamma^2)$
ϵ^1	$e_1 = \gamma$	$\frac{1}{2}C_{11}\gamma^2$
ϵ^2	$e_2 = \gamma$	$\frac{1}{2}C_{22}\gamma^2$
ϵ^3	$e_3 = \gamma$	$\frac{1}{2}C_{33}\gamma^2$
ϵ^4	$e_1 = 2\gamma, e_2 = -\gamma, e_3 = -\gamma$	$\frac{1}{2}(4C_{11} - 4C_{12} - 4C_{13} + C_{22} + 2C_{23} + C_{33})\gamma^2$
ϵ^5	$e_1 = -\gamma, e_2 = 2\gamma, e_3 = -\gamma$	$\frac{1}{2}(C_{11} - 4C_{12} + 2C_{13} + 4C_{22} - 4C_{23} + C_{33})\gamma^2$
ϵ^6	$e_1 = -\gamma, e_2 = -\gamma, e_3 = 2\gamma$	$\frac{1}{2}(C_{11} + 2C_{12} - 4C_{13} + C_{22} - 4C_{23} + 4C_{33})\gamma^2$
ϵ^7	$e_4 = \gamma$	$\frac{1}{2}C_{44}\gamma^2$
ϵ^8	$e_5 = \gamma$	$\frac{1}{2}C_{55}\gamma^2$
ϵ^9	$e_6 = \gamma$	$\frac{1}{2}C_{66}\gamma^2$

TABLE II: Calculated lattice parameters (a , b and c , in Å), volumes of unit cell (V , in Å³), and bulk modulus (B , in GPa) of orthorhombic OsB₂, along a comparison with other theoretical work and available experimental data.

Property	This work		Previous ^a		Experiment
	LDA	GGA	LSDA	LSDA+SO	
a	4.6444	4.7049	4.6433	4.6383	4.6832 ^b
b	2.8505	2.8946	2.8467	2.8437	2.8717 ^b
c	4.0464	4.0955	4.0432	4.0388	4.0761 ^b
V	53.57	55.78	53.44	53.27	54.82 ^b
B	336.1	303.45	364.7	385.4	365-395 ^c

^asee Ref.33

^bsee Ref.32

^csee Ref.17

TABLE III: Calculated elastic constants of orthorhombic OsB₂. Note that a relaxation of the atomic positions was carried out. All values are in units of GPa.

C_{11}	C_{12}	C_{13}	C_{22}	C_{23}	C_{33}	C_{44}	C_{55}	C_{66}
597.0	198.1	206.1	581.2	142.6	825.0	70.1	212.0	201.3

Figure Captions

- FIG 1: The ball-and-stick model for structure of orthorhombic OsB₂. (a) The unit cell containing a single formula unit. Two Os atoms at Wyckoff positions of 2a: Os1 ($\frac{1}{4}, \frac{1}{4}, z$) and Os2 ($\frac{3}{4}, \frac{3}{4}, -z$). Four B atoms at Wyckoff positions of 4f: B1 ($u, \frac{1}{4}, v$), B2 ($-u + \frac{1}{2}, \frac{1}{4}, v$), B3 ($-u, \frac{3}{4}, -v$), and B4 ($u + \frac{1}{2}, \frac{3}{4}, -v$). (b) The supercell repeated in three dimensions by $2 \times 2 \times 2$, in order to illustrate the layers in z (or c)-direction. Os atoms are shown as dark gray balls and boron atoms as light gray balls.
- FIG 2: Calculated pressure versus fractional unit cell volume for OsB₂, along a comparison with available experiment data.
- FIG 3: Electronic band structure along the high-symmetry direction of the Brillouin zone for OsB₂. High-symmetry points are labeled as the following [40]: $\Gamma = (0.0, 0.0, 0.0)$, $Y = (0.0, 0.5, 0.0)$, $S = (0.5, 0.5, 0.0)$, $X = (0.5, 0.0, 0.0)$, and $Z = (0.0, 0.0, 0.5)$. The zero of energy is set as the Fermi level and shown in dotted line.
- FIG 4: (Color online) Total, site and angular momentum-decomposed density of states (DOS) of OsB₂.
- FIG 5: Charge density at the equilibrium lattice parameters of OsB₂, along the lines between (a) Os and B atoms, (b) Os and Os atoms, and (c) B and B atoms.
- FIG 6: Contours of the charge density at the equilibrium lattice parameters of OsB₂, in the planes (a) with normal vector along $\langle 100 \rangle$ and central point at Os1 atom, (b) with normal vector along $\langle 100 \rangle$ and central point at B1 atom, (c) with normal vector along $\langle 010 \rangle$ and central point at Os1 atom, (d) with normal vector along $\langle 001 \rangle$ and central point at Os1 atom, (e) with normal vector along $\langle 001 \rangle$ and central point at B1 atom, and (f) through B1, B2, B3 and B4 atoms. Charge density is in an increment of $0.1 e/\text{\AA}^3$ from 0 to $2.1 e/\text{\AA}^3$ and all distances are in \AA .

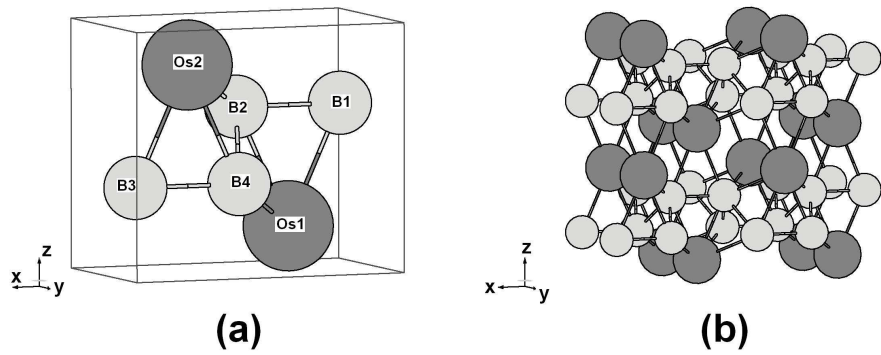


FIG. 1:

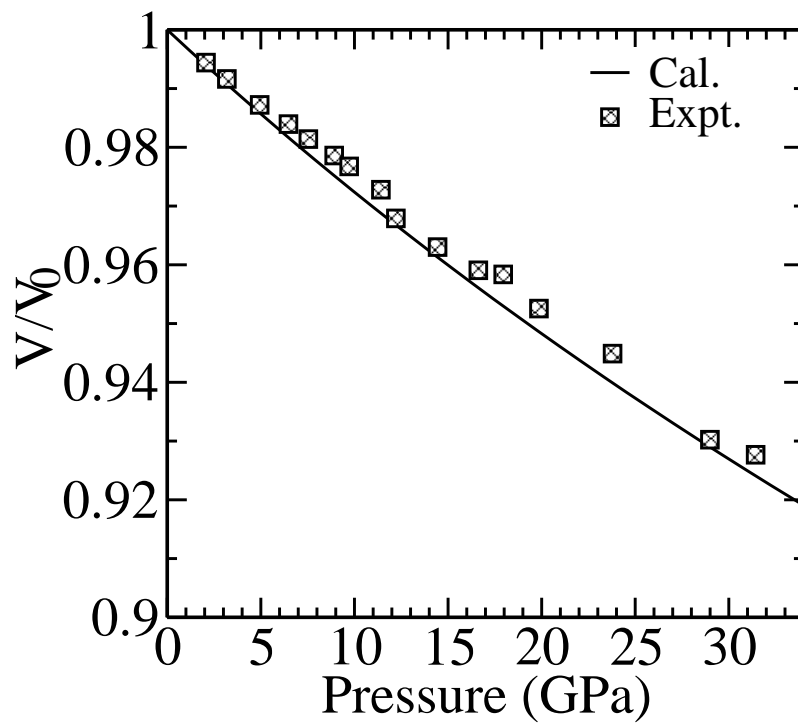


FIG. 2:

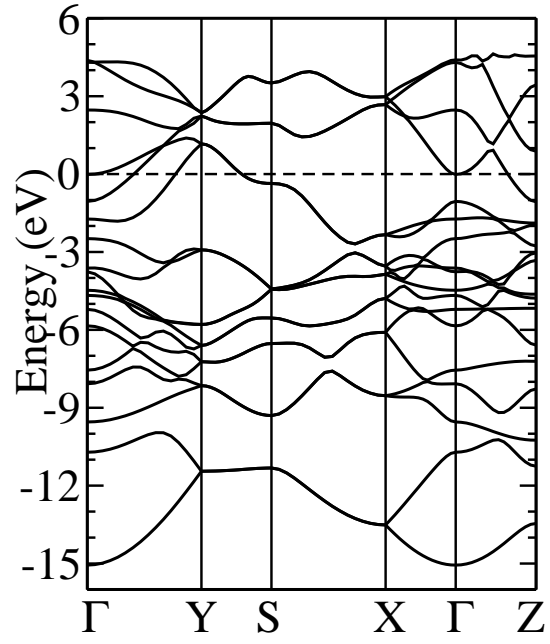


FIG. 3:

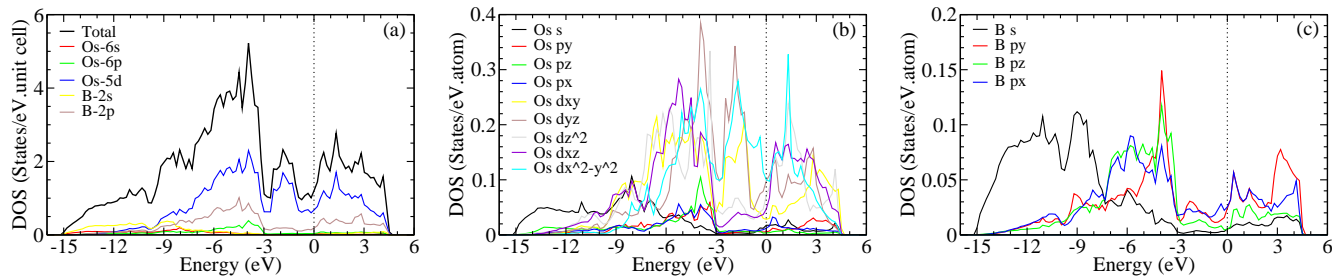


FIG. 4:

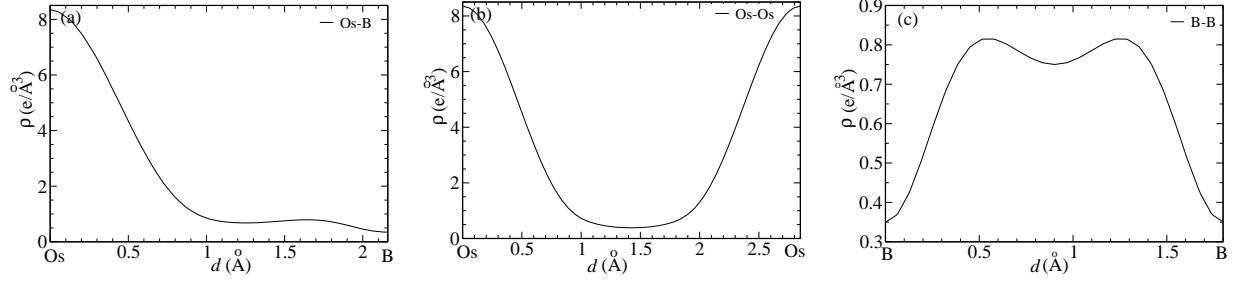


FIG. 5:

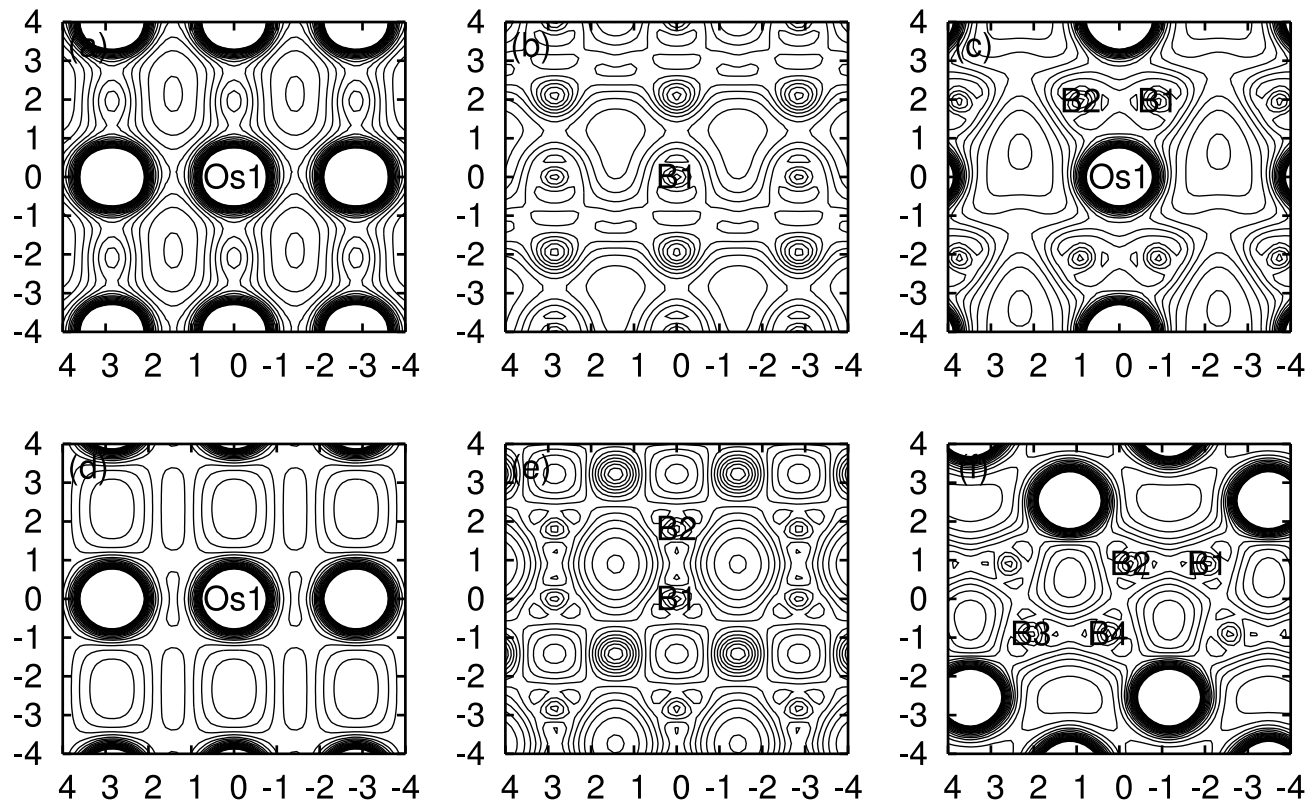


FIG. 6: